ARTICLES

Journal of Semiconductors
(2019) 40, 032201
doi: 10.1088/1674-4926/40/3/032201

Influence of defect states on the performances of planar tin halide perovskite solar cells

Shihua Huang[1, †], Zhe Rui[1], Dan Chi[1], and Daxin Bao[2]

[1]Provincial Key Laboratory of Solid State Optoelectronic Devices, Zhejiang Normal University, Jinhua 321004, China
[2]Hengdian Group DMEGC Magnetics Co., Ltd, Dongyang 322118, China

Abstract: Although tin halide perovskite has shown excellent photoelectric performance, its efficiency of solar cell is low compared with that of lead halide. In order to enhance the efficiency of tin halide perovskite solar cell, a deep understanding of the role of the defects in the perovskite absorption layer and at the electron transport layer (ETL)/absorber or absorber/hole transport layer (HTL) interface is very necessary. In this work, the planar heterojunction-based $CH_3NH_3SnI_3$ perovskite solar cells were simulated with the SCAPS-1D program. Simulation results revealed a great dependence of device efficiency on defect density and interface quality of the perovskite absorber. The defect density at the front interface is critical for high efficiency, and the polarity of the interface charge has a different impact on the device efficiency. Strikingly, an efficiency over 29% was obtained under the moderate simulation conditions.

Key words: simulation; tin halide perovskite; interface defect state; heterojunction solar cell

Citation: S H Huang, Z Rui, D Chi, and D X Bao, Influence of defect states on the performances of planar tin halide perovskite solar cells[J]. *J. Semicond.*, 2019, 40(3), 032201. http://doi.org/10.1088/1674-4926/40/3/032201

1. Introduction

Methylammonium mixed lead halides (MAPbXs), which are known for their excellent optical and electrical properties, have drawn a great deal of attention for photovoltaic applications in recent years[1–4]. MAPbX has unique characteristics, such as large absorption coefficients enabled by direct optical transitions, small exciton binding energies, existence of free carriers, and long carrier diffusion lengths. Therefore, the optoelectronic conversion efficiency of the MAPbX perovskite solar cell (PSC) has been significantly enhanced from 3.8% to 22.1% in a short time span of eight years[5–7]. Although MAPbXs provide many superior performances, the use of the toxic element lead could be problematic for large-scale implementation. Therefore, replacing lead with environment-friendly elements could greatly increase its potential for practical application and production.

Tin halide $MASnI_3$ ($MA = CH_3NH_3$) perovskite solar cells have been intensively investigated for lead-free alternatives[8–10]. $CH_3NH_3SnI_3$ has a narrower band gap of 1.3 eV compared to their Pb-based counterparts (~1.6 eV), which makes it possible to cover a wider range of the visible spectrum, and then a larger short-circuit current (J_{SC}) is expected for $MASnI_3$ PSC. Although $MASnI_3$ PSC has shown excellent performance, its efficiency is still less than 9%[11–13], which can be attributed to several reasons. The easy oxidation of Sn^{2+} to Sn^{4+} causes severe device deterioration in an ambient environment[14]. The low formation energy of Sn vacancies usually leads to high doped hole concentration, which results in severe carrier recombination in the solar cells. Moreover, the functional layers in Sn-based perovskite solar cells, such as hole or electron transport layer, may cause poor energy level alignment and severe interface recombination, which further limit the device performance.

In order to further improve the conversion efficiencies of $MASnI_3$ PSC, it is required to deeply understand the internal electron dynamics and corresponding interfacial engineering, and to clarify the limiting physical mechanism of the conversion efficiency. It is well known that an excellent interface quality is the key factor for a high efficiency PSC due to a strong interface recombination of defect states.

Numerical simulation is now becoming increasingly important for the understanding, design, and optimization of high-efficient solar cells. The simulation method allows an intuitive examination of each parameter in the solar cell and thus identifies the optimal conditions for operating. Up to now, there has been no report concerning the numerical simulation of $MASnI_3$ PSC.

In this paper, influences of defect states in the absorption layer and on the interfaces of absorber/electron transport layer (ETL) or absorber/hole transport layer (HTL) on $MASnI_3$ PSC efficiency are investigated by a one-dimensional device simulation with SCAPS-1D (version 3.3.02) [15, 16]. The SCAPS-1D program is a general solar cell simulation program that is based on Poisson and Continuity equations, and it has been employed to model planar structure perovskite based solar cells due to their structural similarity to thin film solar cells and Wannier type excitons in perovskites[17–20]. In this paper, effects of the defects in the perovskite absorption layer and interface defects of absorber/ETL (or HTL) were deeply investigated. Considering the effects of defect states, a simulated cell efficiency of more than 29% is achieved by optimization of the various parameters. An in-depth understanding of the transport properties can help in improving the efficiency of solar cells and provide a useful guidance to the actual PSC manufacturing.

Correspondence to: S H Huang, huangshihua@zjnu.cn
Received 14 JUNE 2018; Revised 7 JULY 2018.

Table 1. Simulation parameters of Sn-based PSC.

Parameter	TCO	TiO_2 (ETL)	IDL-ETL	$MASnI_3$ (absorber)	IDL-HTL	Spiro-OMeTAD (HTL)
Thickness (nm)	500	200	10	600	10	200
E_g (eV)	3.50	3.20	1.30	1.30	1.30	3.17
χ (eV)	4.00	4.26	4.17	4.17	4.17	2.05
ε_r	9.0	9.0	8.2	8.2	8.2	3.0
μ_n/μ_p ($cm^2/(V{\cdot}s)$)	20/10	20/10	2.0/2.0	2.0/2.0	2.0/2.0	$2/2\times10^{-4}$
N_D (cm^{-3})	2×10^{19}	1×10^{16}	–	–	–	–
N_A (cm^{-3})	–	–	1×10^{15}	1×10^{15}	1×10^{15}	2×10^{18}
N_t (cm^{-3})	1×10^{15}	1×10^{15}	$1\times10^{15-21}$	$1\times10^{11-19}$	$1\times10^{15-21}$	1×10^{15}
N_{it} (cm^{-2})	–	–	$1\times10^{9-15}$	–	$1\times10^{9-15}$	–

2. Device simulation parameters

The simulated PSC structure is the transparent conductive oxide (TCO) glass/TiO_2/$MASnI_3$/Spiro-OMeTAD/metal back contact, and the sunlight is illuminated from TCO glass. TiO_2 acts as ETL, Spiro-OMeTAD as HTL, and $MASnI_3$ as the absorption layer. The absorber is assumed to be fully depleted and the electric field is formed by high densities of electron and hole of TCO and HTL, respectively. In order to simulate a more realistic PSC, we intentionally insert a very thin interface layer in the absorber region with a large number of defect states. The interface defect layer (IDL) is assumed to take into account the interface recombination, and IDL-ETL and IDL-HTL are inserted between ETL/absorber and absorber/HTL layers, respectively. Material parameters were selected from experimental data and theoretical results. The main simulated parameters are listed in Table 1[11, 12, 14, 16, 19–27]. Here, N_A and N_D denote acceptor and donor densities, ε_r is relative permittivity, χ is electron affinity, E_g is band-gap energy, μ_n and μ_p are mobility of electron and hole, N_t is defect density in the film, and D_{it} is interface defect density of ETL/absorber and absorber/HTL. The N_t of IDL was changed from 10^{15} to 10^{21} cm^{-3}, which corresponds to a change in D_{it} from 10^9 to 10^{15} cm^{-2} in case of the thickness of 10 nm for IDL-ETL and IDL-HTL. Considering the high density of the defects and short carrier diffusion length at the interfaces of ETL/absorber and absorber/HTL, it is appropriate to set the thickness of IDL-ETL and IDL-HTL to 10 nm. The following parameters were set to be identical in all layers. Effective densities of states of the conduction band (N_C) and valence band (N_V) are 2.0×10^{18} and 2.0×10^{19} cm^{-3}, respectively. Thermal velocities (v_{th}) of electron and hole were both set to be equal to 10^7 cm/s. The defect energy level is at the center of the band gap, and the energetic distribution is Gaussian with characteristic energy of 0.1 eV. The defect type in TiO_2, $MASnI_3$, and Spiro-OMeTAD thin films is neutral. However, defect types in the interfaces of ETL/absorber and absorber/HTL were set to neutral, donor, and acceptor, respectively. The capture cross section of electron or hole (σ_n or σ_p) is 1.0×10^{-15} cm^2. A flat band was applied to the front and back contacts to prevent a contact potential. The absorption coefficient spectra of ETL and HTL materials were calculated by $\alpha(E) = A_\alpha(h\nu - E_g)^{1/2}$, and the pre-factor A_α was extracted from Ref. [11]. In the simulation, AM 1.5 radiation was used as the illumination source with a power density of 100 mW/cm^3, and the device temperature was set as 300 K.

3. Results and discussion

The influence of the thickness and doping concentration of each layer of PSC on the device performance were extensively investigated[23, 28–30]. The spectral response is a key factor in determining device performance and it is closely related to the device thickness. The short-circuit current density (J_{SC}) increases with the thickness of the perovskite absorption layer and then saturates due to the limit of the carrier diffusion length. The open-circuit voltage (V_{OC}) decreases slightly due to an increased charge recombination in thicker films. With the increase of the HTL (or ETL) layer thickness, the conversion efficiency gradually decreases, which results from a reduction in light absorption. Hence, the optimized thickness of absorber, HTL, and ETL were selected as 600, 200, and 200 nm, respectively.

Because the self-doping process of Sn^{2+} is easily oxidized to Sn^{4+}, the tin-based perovskite exhibits a p-type conductive behavior[25]. Experimental results indicate that the doping level in $MASnI_3$ film can be varied in a range of 10^{14} – 10^{17} cm^{-3}[7, 12]. An appropriate doping concentration of the perovskite absorption layer is beneficial to the improvement of PSC efficiency. When the doping concentration of the absorption layer increases, the built-in electric field in PSC enhances, which improves the separation efficiency of carriers, hence improving the cell performance. Further increasing the doping concentration above 1×10^{18} cm^{-3}, the cell performance deteriorates due to a higher Auger recombination rate. An increase in the recombination rate affects the cell performance greatly and should be avoided effectively. Therefore, combining experiments and simulation results, the suitable doping concentration of the $MASnI_3$ absorption layer was set to 1.0×10^{15} cm^{-3}.

The properties and the amount of defects in the perovskite absorber play a key role in determining device performance, because photogenerated carriers are mainly generated in this layer and the carrier recombination is dominant in determining the V_{OC} of PSC. Therefore, for simplicity, we did not consider the effects of the defects in HTL or ETL. The device performances are improved significantly with the reduction of the defect density N_t in $MASnI_3$ thin film, as shown in Fig. 1. When the N_t in $MASnI_3$ is lower than 1×10^{12} cm^{-3}, the PSC efficiency (Eff) is 36% without considering the influence of interface defects between the interfaces of the ETL/absorber and absorber/HTL. Further analysis shows that N_t in $MASnI_3$ is lower than 1×10^{10} cm^{-3}, Eff is no longer increased and reaches its maximum value (40.5%, no display in Fig. 1). For the solar cell of a single homogenous junction with $E_g = 1.34$ eV, the theoretical Eff limit by the Shockley–Queisser theory is 33.7%[31, 32]. For the simulated perovskite solar cell, the band-gap energy of ETL (TiO_2), the absorber layer ($MASnI_3$), and HTL (Spiro-OMeTAD) are 3.20, 1.30, and 3.17 eV, respectively. Therefore,

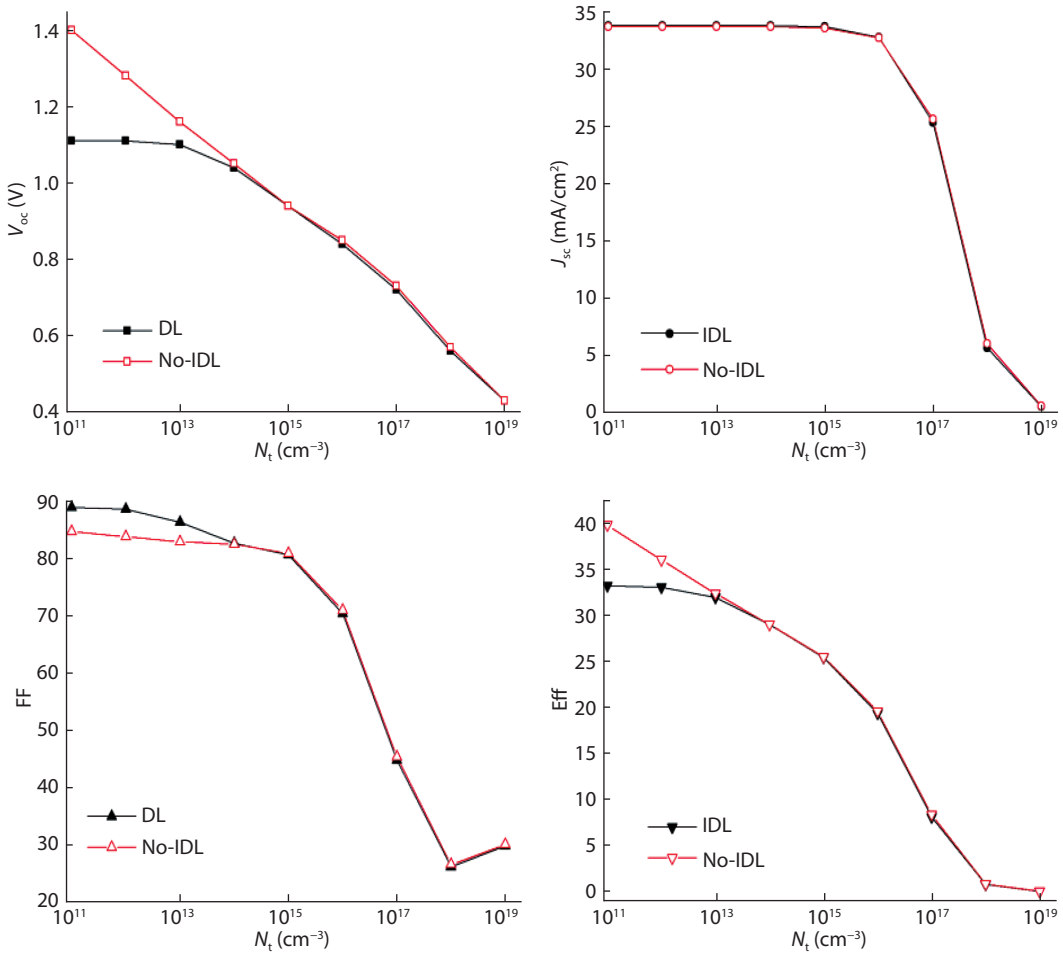

Fig. 1. (Color online) Solar cell parameters of PSC with (or without) IDL as a function of defect density N_t in $MASnI_3$ thin film.

thesimulatedsolarcellcanbeapproximatelyregardedasadouble junction solar cell with a theoretical Eff limit of 44.3%[33].

Without considering the influence of the interface defect, the V_{OC} is almost linearly reduced with the exponential increase of N_t. V_{OC} is given by

$$V_{OC} = \frac{kT}{q}\ln\left(\frac{I_L}{I_0}+1\right), \tag{1}$$

where q is the electronic charge, k is the Boltzmann constant, T is the temperature, I_L is the light-generated current, and I_0 is the saturation current. While I_L typically has a small variation, the key factor affecting V_{OC} is I_0, since this may vary by orders of magnitude. The saturation current (I_0) depends on recombination in the solar cell, and can be written by

$$I_0 = AkTn_i^2\left(\frac{\mu_n}{L_nN_A}+\frac{\mu_p}{L_pN_D}\right), \tag{2}$$

where A is the quality factor, n_i is the intrinsic carrier concentration, and L_n (L_p) is the electron (hole) diffusion length. The most important factor affecting I_0 is diffusion length, which is given by

$$L_{n,p} = \sqrt{\frac{\mu_{n,p}kT}{q}\frac{1}{\sigma_{n,p}v_{th}N_t}}. \tag{3}$$

According to Eqs. (1)–(3), the V_{OC} is almost linearly decreased with the exponential increase of N_t, which is consistent with the simulation results. The J_{SC} has almost no change in the case of N_t lower than 1×10^{16} cm^{-3}, however, J_{SC} decreases significantly with the further increase of N_t, as shown in Fig. 1. For a low N_t, L_n (or L_p) is larger than the absorber thickness, thus the impact of N_t to J_{SC} is rather small. However, for a large N_t (for example, 1×10^{16} cm^{-3}), L_n (or L_p) is smaller than the absorber thickness, so J_{SC} decreases rapidly with the increase of N_t. In fact, a low trap-assisted recombination rate in perovskite thin film has been reported by Herz *et al.*[34], therefore, the suitable defect density in $MASnI_3$ thin film can be set to 1×10^{14} cm^{-3}.

In case of considering the influence of an interface defect, the interface defect density ($D_{it\text{-}ETL}$ or $D_{it\text{-}HTL}$) was set to a very low value ~1×10^{9} cm^{-2}. When N_t is larger than 1×10^{14} cm^{-3}, the insertion of the interface defect layer with a low D_{it} has almost no influence on the PSC performance, as shown in Fig. 1. As N_t is lower than 1×10^{14} cm^{-3}, the presence of interface defects deteriorates the PSC performance, which is caused by the interface recombination loss. Of course, if D_{it} was set to a larger value (for example, 1×10^{14} cm^{-2}), the interface defect has an important influence on PSC performance in case of any value of N_t.

The interface quality has a decisive influence on the efficiency of thin film solar cell because the presence of interface defects can lead to high levels of recombination. In real devices, it is difficult to characterize the interface defect dens-

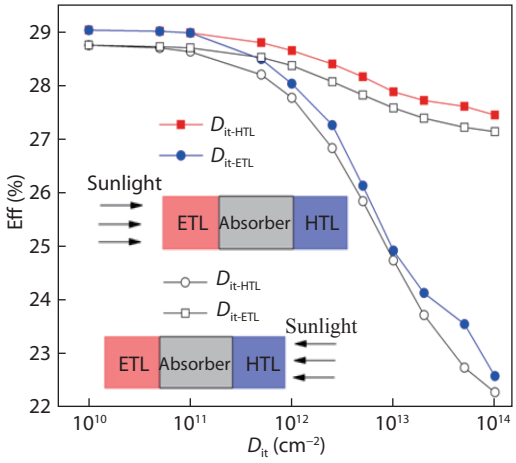

Fig. 2. (Color online) Efficiency of PSC with neutral interface defects as a function of interface defect density.

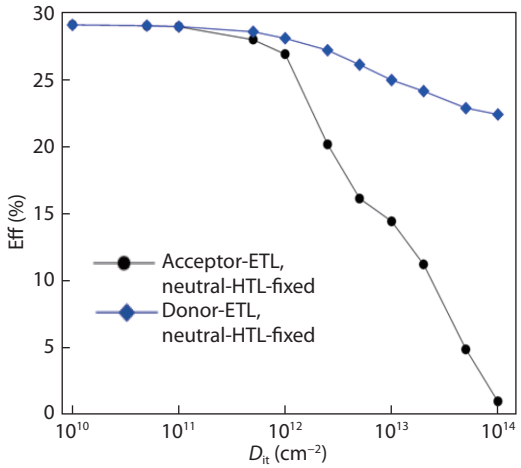

Fig. 3. (Color online) Efficiency of PSC with donor (or acceptor) interface defects as a function of interface defect density.

ity and recombination rate. In the simulation, the influence of an interface state on the device performance can be revealed by drastically changing the interface defect density. Here, two interface defects are considered, and they are the interface defect $D_{it\text{-}ETL}$ located between the ETL and the absorber (TiO_2/$MASnI_3$) and the interface defect $D_{it\text{-}HTL}$ between the absorber and HTL ($MASnI_3$/HTL). Two D_{it} values change from 10^{10} to 10^{14} cm^{-3}. In the perovskite absorption layer, the defect type (neutral, donor, or acceptor) has almost no influence on PSC performances, and the simulated results were not shown here. However, different defect types of $D_{it\text{-}ETL}$ and $D_{it\text{-}HTL}$ were considered, and their influences on PSC were investigated in depth.

For the simplicity, the neutral defect type was analyzed at first. The efficiencies of PSC with different defect densities at ETL/absorber and absorber/HTM interfaces were demonstrated, as shown in Fig. 2. As $D_{it\text{-}ETL}$ or $D_{it\text{-}HTL}$ was changed from 10^{10} to 10^{14} cm^{-2}, the other parameter $D_{it\text{-}HTL}$ or $D_{it\text{-}ETL}$ was fixed at 10^{10} cm^{-2}. The Eff decreases from 29.02% to 27.44% when $D_{it\text{-}HTL}$ increases from 10^{10} to 10^{14} cm^{-2}. However, the Eff decreases from 29.02% to 22.57% with the increase of $D_{it\text{-}ETL}$ from 10^{10} to 10^{14} cm^{-2}. Therefore, the interface quality at the absorber/HTL interface has a greater impact on PSC efficiencies than that at the ETL/absorber interface. When the sunlight changes its incident direction, namely, from the HTL to the ETL, the simulated results are just the opposite, as illustrated in Fig. 2. These results indicate that the interface quality of the sunlight incident side of PSC is far more important than that of the back side.

The difference is caused by the collection probability of photogenerated carriers, which is that a light generated carrier absorbed in a certain region of the device will be collected by the p-n junction and therefore contribute to the light-generated current. Similarly, if the carrier is generated more than a diffusion length away from the junction, then the collection probability of this carrier is quite low. If the carrier is generated closer to a region such as a surface with high recombination, then the carrier will be recombined. For high absorption coefficient of the pervoskite absorber, the number of photogenerated electron-hole pairs at the light irradiation side is high at the surface and significantly becomes small toward the back side. The presence of the localized recombination site, such as a surface or interface, has a stronger influence on the collection probability than a less severe localized recombination site. Therefore, as the sunlight irradiates from the side of ETL/absorber, the higher excess carrier density will be generated, which leads to a larger recombination rate at ETL/absorber than that at absorber/HTL. Thus, the interface defect at ETL/absorber has stronger influence on device performance than absorber/HTL. On the contrary, if the device is irradiated from the HTM side, the defect density of the absorber/HTM interface has a strong impact on the device performance, as shown in Fig. 2. In order to enhance the efficiency of the perovskite solar cell, improving the interface quality of the front side is much more important than that of the back side.

We have discussed the behavior of the interface with neutral defects, next we will analyze the impacts of the interface with donor or acceptor defects on PSC performance. If $D_{it\text{-}HTL}$ was fixed at 10^{10} cm^{-2} with neutral defects, the dependence of device efficiency on $D_{it\text{-}ETL}$ with different defect type was given in Fig. 3. When the defect type of $D_{it\text{-}ETL}$ is neutral or donor, the influence of interface defects on device efficiency is the same, and the Eff decreases from 29.02% to 22.50% with the increase of $D_{it\text{-}ETL}$ from 10^{10} to 10^{14} cm^{-2}. However, in the case of acceptor defects, the Eff drops sharply from 29.02% to 0.96% when $D_{it\text{-}ETL}$ increases from 10^{10} to 10^{14} cm^{-2}, which indicates that $D_{it\text{-}ETL}$ with acceptor defects has a far more important influence on device efficiency than $D_{it\text{-}ETL}$ with neutral or donor defects. Similarly, the impact of $D_{it\text{-}HTL}$ with donor defects on device efficiency is much stronger than that of $D_{it\text{-}HTL}$ with neutral or acceptor defects (not shown in this paper).

The further investigations on the band bending and carrier recombination were shown in Fig. 4. In order to analyze only the band bending and recombination at the interfaces of ETL/absorber and absorber/HTL, the horizontal axis of Fig. 4 starts from 0.2 μm (the thickness of ETL) and ends at 0.82 μm (IDL-ETL (0.01 μm) + absorber (0.6 μm) + IDL-HTL (0.01 μm)). As $D_{it\text{-}ETL}$ with acceptor defects increases, the reduction of the band bending is obviously enhanced, as shown in Fig. 4(a). However, in case of $D_{it\text{-}ETL}$ with donor (or neutral) defects, the interface defect density has almost no influence on band bending, as shown in Fig. 4(b). The band bending affects the photo-generated carrier flow, which leads to the decrease in V_{OC} and deterioration of device performance. The dependences of the interface defect type and defect density on

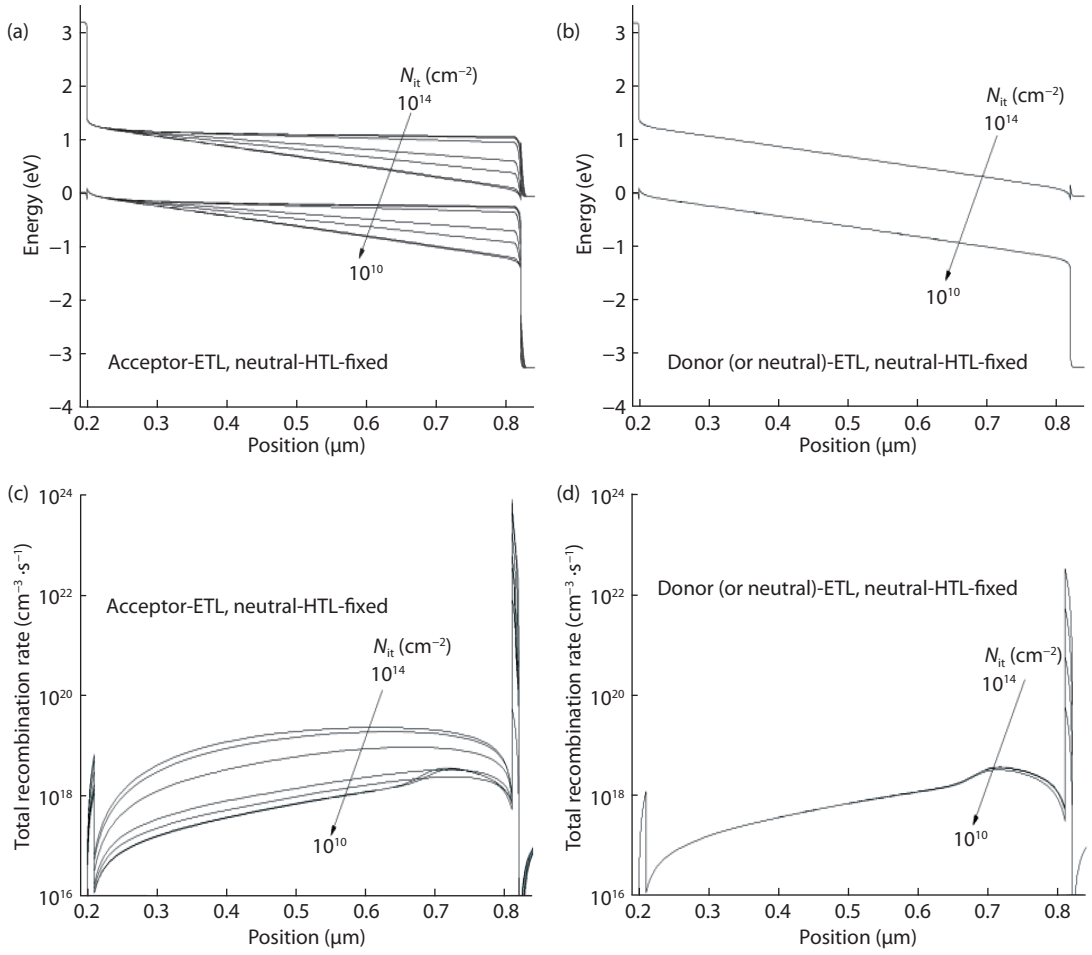

Fig. 4. Distributions of total recombination and energy band in the cell thickness direction for varying interface defect density.

carrier recombination rate are also shown in Figs. 4(c) and 4(d). Similar to the influence on band bending, $D_{it\text{-}ETL}$ with acceptor defects has a much greater impact on recombination rate than $D_{it\text{-}ETL}$ with donor (or neutral) defects.

When interface defect states of the n-type-ETL/p-type-absorber or p-type-absorber/n-type-HTL heterojunction are occupied, charges are trapped at the interface in the space charge region of the heterojunction. As the defect type of $D_{it\text{-}ETL}$ is donor or neutral, the space charge region is not significantly affected, and the electric field extends up to the neutral region of the perovskite absorber with the increase of $D_{it\text{-}ETL}$. However, for $D_{it\text{-}ETL}$ with acceptor defects, the trapped charges prevent the extension of the space charge region into the absorber since the polarity of the interface charge is the same as the polarity of the majority carrier of the perovskite absorber. Therefore, the band bending in the absorber is reduced, which results in a lowering of the effective barrier and consequently a decrease in V_{OC}. In addition, a reduction of the band bending causes an enhancement of the majority carrier concentration at the interface, which leads to an increased recombination probability. Similarly, $D_{it\text{-}HTL}$ with donor defects has a much greater impact on the band bending and recombination rate than $D_{it\text{-}HTL}$ with acceptor (or neutral) defects.

In the actual preparation process of Sn-based perovskite solar cells, some divalent Sn compounds, for example, SnF_2, as an additive, can be used as Sn vacancy suppressors to reduce the defect density in the perovskite absorber and improve device performance[35, 36]. In order to reduce the interface defect density at the absorber/ETL (or HTL), energy band matching between the absorber layer and ETL (or HTL) and composition engineering (such as mixing of the monovalent cations) have proven to be an effective way to tailor the properties of perovskites and enhance the performance of PSCs[37, 38].

4. Conclusion

The planar heterojunction $CH_3NH_3SnI_3$ solar cell was simulated with one-dimensional device simulator SCAPS, which is widely used in inorganic thin film solar cells. The defects in the perovskite absorber and at the ETL/absorber or absorber/HTL interface were deeply investigated. In the case of defect density in a perovskite absorber lower than 1×10^{16} cm^{-3}, J_{SC} has almost no change and high efficiency (> 19.0%) can be obtained. The absorber interface density at the sunlight incident side is a decisive factor for efficiency due to the high absorption coefficient of the pervoskite absorber. The defect density at the ETL/absorber interface with acceptor defects has a far more important influence on device efficiency than that with neutral or donor defects. Similarly, the impact of the defect density at the absorber/HTL interface with donor defects on device efficiency is much stronger than that with neutral or acceptor defects. The polarity of the interface charge has a different impact on the band bending and recombination rate. Considering the effects of defect states, a simulated cell efficiency of more than 29% is achieved by optimization of the various parameters, which highlights the great potential of perovskite in achieving high efficiency. The simulation based on this study will be useful for further understanding of device operation and efficiency improvement.

Acknowledgements

The author would like to thank Professor Marc Burgelman, Department of Electronics and Information Systems, University of Gent for the development of the SCAPS software package and allowing its use.

This work was supported by the Zhejiang Provincial Natural Science Foundation of China (No. LY17F040001), the Technology Development Project Program of Hengdian Group DMEGC Magnetics Co., Ltd (No. 2016330001002138), the Open Project Program of Surface Physics Laboratory (National Key Laboratory) of Fudan University (No. KF2015_02), and the Open Project Program of National Laboratory for Infrared Physics, Chinese Academy of Sciences (No. M201503).

References

[1] Dou L, Yang Y M, You J, et al. Solution-processed hybrid perovskite photodetectors with high detectivity. Nat Commun, 2014, 5, 5404

[2] Zhu H, Fu Y, Meng F, et al. Lead halide perovskite nanowire lasers with low lasing thresholds and high quality factors. Nat Mater, 2015, 14, 636

[3] Stoumpos C C, Kanatzidis M G. The renaissance of halide perovskites and their evolution as emerging semiconductors. Acc Chem Res, 2015, 48, 2791

[4] Stoumpos C C, Kanatzidis M G. Halide perovskites: poor man's high-performance Semiconductors. Adv Mater, 2016, 28, 5778

[5] Kojima A, Teshima K, Shirai Y, et al. Organometal halide perovskites as visible-light sensitizers for photovoltaic cells. J Am Chem Soc, 2009, 131, 6050

[6] Saliba M, Matsui T, Seo J Y, et al. Cesium-containing triple cation perovskite solar cells: improved stability, reproducibility and high efficiency. Energy Environ Sci, 2016, 9, 1989

[7] Green M A, Hishikawa Y, Warta W, et al. Solar cell efficiency tables (version 50). Prog Photovolt Res Appl, 2017, 25, 668

[8] Hao F, Stoumpos C C, Guo P, et al. Solvent-mediated crystallization of $CH_3NH_3SnI_3$ films for heterojunction depleted perovskite solar cells. J Am Chem Soc, 2015, 137, 11445

[9] Yokoyama T, Cao D H, Stoumpos C C, et al. Overcoming short-circuit in lead-free $CH_3NH_3SnI_3$ perovskite solar cells via kinetically controlled gas–solid reaction film fabrication process. J Phys Chem Lett, 2016, 7, 776

[10] Handa T, Yamada T, Kubota H, et al. Photocarrier recombination and injection dynamics in long-term stable lead-free $CH_3NH_3SnI_3$ perovskite thin films and solar cells. J Phys Chem C, 2017, 121, 16158

[11] Noel N K, Stranks S D, Abate A, et al. Lead-free organic–inorganic tin halide perovskites for photovoltaic applications. Energy Environ Sci, 2014, 7, 3061

[12] Hao F, Stoumpos C C, Cao D H, et al. Lead-free solid-state organic–inorganic halide perovskite solar cells. Nat Photonics, 2014, 8, 489

[13] Zhao Z, Gu F, Li Y, et al. Mixed-organic-cation tin iodide for lead-free perovskite solar cells with an efficiency of 8.12%. Adv Sci, 2017, 4, 1700204

[14] Gagliardi A, Maur M A, Gentilini D, et al. The real TiO_2/HTM interface of solid-state dye solar cells: role of trapped states from a multiscale modelling perspective. Nanoscale, 2015, 7, 1136

[15] Niemegeers A, Burgelman M. Numerical modelling of AC-characteristics of CdTe and CIS solar cells. 25th IEEE Photovoltaic Specialists Conference, Washington DC, 1996

[16] Burgelman M. Modelling polycrystalline semiconductor solar cells. Thin Solid Films, 2000, 527, 361

[17] Zhou H, Chen Q, Li G, et al. Interface engineering of highly efficient perovskite solar cells. Science, 2014, 345, 542

[18] Edri E, Kirmayer S, Mukhopadhyay S, et al. Elucidating the charge carrier separation and working mechanism of $CH_3NH_3PbI_{3-x}Cl_x$ perovskite solar cells. Nat Commun, 2014, 5, 3461

[19] Minemoto T, Murata M. Device modeling of perovskite solar cells based on structural similarity with thin film inorganic semiconductor solar cells. J Appl Phys, 2014, 116, 054505

[20] Minemoto T, Murata M. Theoretical analysis on effect of band offsets in perovskite solar cells. Sol Energy Matter Sol Cells, 2015, 133, 8

[21] Giorgi G, Yamashita K. Organic–inorganic halide perovskites: an ambipolar class of materials with enhanced photovoltaic performances. J Mater Chem A, 2015, 3, 8981

[22] Zhang Q, Dandeneau C S, Zhou X, et al. ZnO nanostructures for dye-sensitized solar cells. Adv Mater, 2009, 21, 4087

[23] Liu F, Zhu J, Wei J, et al. Numerical simulation: toward the design of high-efficiency planar perovskite solar cells. Appl Phys Lett, 2014, 104, 253508

[24] Hossain M I, Alharbi F H, Tabet N. Copper oxide as inorganic hole transport material for lead halide perovskite based solar cells. Sol Energy, 2015, 120, 370

[25] Umari P, Mosconi E, Angelis F D. Relativistic GW calculations on $CH_3NH_3PbI_3$ and $CH_3NH_3SnI_3$ perovskites for solar cell applications. Sci Report, 2014, 34, 4467

[26] Khaliq A, Xue F L, Varahramyan K. Numerical simulation of spin coated P_3HT organic thin film transistors with field dependent mobility and distributed contact resistance. Microelectron Eng, 2009, 86, 2312

[27] Chen A, Zhu K, Shao Q, et al. Understanding the effects of TCO work function on the performance of organic solar cells by numerical simulation. Semicond Sci Technol, 2016, 31, 065025

[28] Toshniwal A, Jariwala A, Kheraj V, et al. Numerical simulation of tin based perovskite solar cell: effects of absorber parameters and hole transport materials. J Nano-Electron Phys, 2017, 9, 03038

[29] Karimi E, Ghorashi S M B. Investigation of the influence of different hole-transporting materials on the performance of perovskite solar cells. Optik, 2017, 130, 650

[30] Nakanishi A, Takiguchi Y, Miyajima S. Device simulation of $CH_3NH_3PbI_3$ perovskite/heterojunction crystalline silicon monolithic tandem solar cells using an n-type a-Si:H/p-type μc-$Si_{1-x}O_x$:H tunnel junction. Phys Status Solidi A, 2016, 213, 1997

[31] Shockley W, Queisser H J. Detailed balance limit of efficiency of p-n junction solar cells. J Appl Phys, 1961, 32, 510

[32] Rühle S. Tabulated values of the Shockley-Queisser limit for single junction solar cells. Sol Energy, 2016, 130, 139

[33] Marti A, Araújo G L. Limiting efficiencies for photovoltaic energy conversion in multigap systems. Sol Energy Mater Sol Cells, 1996, 43, 203

[34] Wehrenfennig C, Eperon G E, Johnston M B, et al. High charge carrier mobilities and lifetimes in organolead trihalide perovskites. Adv Mater, 2014, 26, 1584

[35] Kontos A G, Kaltzoglou A, Siranidi E, et al. Structural stability, vibrational properties, and photoluminescence in $CsSnI_3$ perovskite upon the addition of SnF_2. Inorg Chem, 2017, 56, 84

[36] Yokoyama T, Song T B, Cao D H, et al. The origin of lower hole carrier concentration in methylammonium tin halide films grown by vapor-assisted solution process. ACS Energy Lett, 2017, 2, 22

[37] Ke W, Stoumpos C C, Logsdon J L, et al. TiO_2–ZnS cascade electron transport layer for efficient formamidinium tin iodide perovskite solar cells. J Am Chem Soc, 2016, 138, 14998

[38] Xu X, Chueh C C, Yang Z, et al. Ascorbic acid as an effective antioxidant additive to enhance the efficiency and stability of Pb/Sn-based binary perovskite solar cells. Nano Energy, 2017, 34, 392